

- 47 Pasinetti, G.M. et al. (1994) *J. Comp. Neurol.* 339, 387–400  
 48 Wong, P. et al. (1993) *J. Biol. Chem.* 268, 5021–5031  
 49 Garden, G.A., Bothwell, M. and Rubel, E.W. (1991) *J. Neurobiol.* 22, 590–604  
 50 D'Mello, S.R. and Galli, C. (1993) *NeuroReport* 4, 355–358  
 51 Wießner, C. et al. (1993) *Mol. Brain Res.* 20, 345–352  
 52 Schreiber, S.S. et al. (1993) *Neurosci. Lett.* 153, 17–20  
 53 May, P.C. and Finch, C.E. (1992) *Trends Neurosci.* 15, 391–396  
 54 Wyllie, A.H. and Duvall, E. (1992) in *Oxford Textbook of Pathology*, Vol. 1 (McGee, J.O'D., Isaacson, P.G. and Wright, N.A., eds), pp. 141–157, Oxford University Press  
 55 Steller, H. (1995) *Science* 267, 1445–1449  
 56 Thompson, C.B. (1995) *Science* 1456–1462  
 57 Evans, V.G. (1993) *Cell Biol. Int.* 17, 461–476  
 58 Eastman, A. (1993) *Toxicol. Appl. Pharmacol.* 121, 160–164  
 59 Gold, R. et al. (1994) *Lab. Invest.* 71, 219–225  
 60 Goto, K. et al. (1990) *Brain Res.* 534, 299–302  
 61 Sloviter, R.S., Dean, E. and Neubort, S. (1993) *J. Comp. Neurol.* 330, 337–351  
 62 Wijsman, J.H. et al. (1993) *J. Histochem. Cytochem.* 41, 7–12  
 63 Gold, R. et al. (1993) *J. Histochem. Cytochem.* 41, 1023–1030  
 64 Gavrieli, Y., Sherman, Y. and Ben-Sasson, A.J. (1992) *J. Cell Biol.* 119, 493–501  
 65 Kressel, M. and Groscurth, P. (1994) *Cell Tissue Res.* 278, 549–556  
 66 Pollard, H. et al. (1994) *NeuroReport* 5, 1053–1055  
 67 MacManus, J.P. et al. (1994) *NeuroReport* 5, 493–496  
 68 Heron, A. et al. (1993) *J. Neurochem.* 61, 1973–1976  
 69 Nitatori, T. et al. (1995) *J. Neurosci.* 15, 1001–1011  
 70 Leppin, C. et al. (1992) *Brain Res.* 581, 168–170  
 71 Deshpande, J. et al. (1992) *Exp. Brain Res.* 88, 91–105  
 72 Loo, D.T. et al. (1993) *Proc. Natl. Acad. Sci. USA* 90, 7951–7955  
 73 Forloni, G. et al. (1993) *NeuroReport* 4, 523–526  
 74 Su, J.H. et al. (1994) *NeuroReport* 5, 2529–2533  
 75 Lassmann, H. et al. (1995) *Acta Neuropathol.* 89, 35–41  
 76 Portera-Cailliau, C. et al. (1995) *J. Neurosci.* 15, 3775–3787  
 77 Colotta, F. et al. (1992) *J. Biol. Chem.* 267, 18278–18283  
 78 Liu, Z-G. et al. (1994) *Nature* 367, 281–284  
 79 Shi, Y. et al. (1992) *Science* 257, 212–214  
 80 Liu, P.K. et al. (1994) *Ann. Neurol.* 36, 566–576  
 81 Wahlestedt, C. et al. (1993) *Nature* 363, 260–263  
 82 Donehower, L.A. et al. (1992) *Nature* 356, 215–221  
 83 Lowe, S.W. et al. (1993) *Nature* 362, 847–849  
 84 Clarke, A.R. et al. (1993) *Nature* 362, 849–852  
 85 Davies, A.M. and Rosenthal, A. (1994) *Neurosci. Lett.* 182, 112–114  
 86 Crumrine, R.C., Thomas, A.L. and Morgan, P.F. (1994) *J. Cereb. Blood Flow Metab.* 14, 887–891  
 87 Wood, K.A. and Youle, R.J. *J. Neurosci.* (in press)  
 88 Estus, S. et al. (1994) *J. Cell Biol.* 127, 1717–1727  
 89 Ham, J. et al. (1995) *Neuron* 14, 927–939  
 90 Eisenberg, O. et al. (1994) *Soc. Neurosci. Abstr.* 20, 1268  
 91 Zhang, P. et al. (1992) *Neuroscience* 46, 19–21  
 92 Anderson, A.J., Cummings, B.J. and Cotman, C.W. (1994) *Exp. Neurol.* 125, 286–295  
 93 Harrison, P.J. et al. (1993) *Neuropathol. Appl. Neurobiol.* 19, 10–21

## Receptive-field dynamics in the central visual pathways

Gregory C. DeAngelis, Izumi Ohzawa and Ralph D. Freeman

**Neurons in the central visual pathways process visual images within a localized region of space, and a restricted epoch of time. Although the receptive field (RF) of a visually responsive neuron is inherently a spatiotemporal entity, most studies have focused exclusively on spatial aspects of RF structure. Recently, however, the application of sophisticated RF-mapping techniques has enabled neurophysiologists to characterize RFs in the joint domain of space and time. Studies that use these techniques have revealed that neurons in the geniculostriate pathway exhibit striking RF dynamics. For a majority of cells, the spatial structure of the RF changes as a function of time; thus, these RFs can be characterized adequately only in the space-time domain. In this review, the spatiotemporal RF structure of neurons in the lateral geniculate nucleus and primary visual cortex is discussed.**

*Trends Neurosci.* (1995) 18, 451–458

THE RECEPTIVE FIELD (RF) is defined classically as the area of visual space within which the discharge of a neuron can be influenced<sup>1</sup>. The RF is a central construct in the conceptual and analytical framework that is used by neurophysiologists to study the function of visually responsive neurons, because it characterizes the transformation between the visual image and neuronal activity. Although traditional textbook depictions (for example, Fig. 1, left) define the RF in spatial coordinates only, it is inherently a function of both space and time. Thus, to describe adequately how a neuron processes the visual image, its RF must be characterized in the joint space-time domain.

In recent years, the development of powerful RF-mapping techniques, based on white-noise analysis, has facilitated the spatiotemporal characterization of

RFs for neurons in the geniculo-cortical processing stream<sup>2,3,5,11–15</sup>. Results that were obtained using this approach have resolved some longstanding questions concerning the origin of neuronal response properties, such as direction selectivity. In addition, because these studies have revealed new aspects of RF structure, they pose new challenges for understanding and modeling the neural circuitry of the early visual pathways.

### The geniculostriate processing stream

In the mammalian visual system, information is processed sequentially along the pathway from the retina through the lateral geniculate nucleus (LGN) to the primary (or striate) visual cortex. Spiking neurons along this pathway exhibit one of three main RF configurations (Fig. 1). For retinal ganglion cells and

Gregory C. DeAngelis, Izumi Ohzawa and Ralph D. Freeman are in the Group in Vision Science, School of Optometry, University of California, Berkeley, CA 94720-2020, USA.

LGN neurons, the RF has an approximately circular, center-surround organization<sup>16,17</sup>. Two primary configurations are observed: one in which the RF center is responsive to bright stimuli ('ON-center'; see Fig. 1A), and the surround is responsive to dark stimuli; and another ('OFF-center') in which the respective polarities are reversed. Simple cells, which receive most of the geniculate input to the primary visual cortex, have spatially oriented RFs (Fig. 1B), with alternating elongated subregions that are responsive to bright or dark stimuli<sup>12,18</sup>. It is generally thought that simple-cell RFs are formed from an array of LGN RFs (Refs 18 and 19), although intracortical inhibitory mechanisms might also play a role in generating the stimulus selectivity of these cells<sup>20</sup>. Complex cells, the other major physiological cell type in the striate cortex, respond to both bright and dark stimuli that are placed anywhere within their RFs (Refs 18 and 21) (Fig. 1C). These RFs are thought to be formed through a non-linear combination of subunits that resemble simple cells<sup>9,18,21,22</sup>.

### Approaches to RF mapping

The response of a neuron to monocular visual stimulation can generally be described as a function of three variables: two dimensions of space,  $x$  and  $y$  (that is, retinal coordinates), and time,  $t$ . Clearly, extensive collection of data is required to map a cell's RF, with high resolution, in the  $x$ - $y$ - $t$  domain, especially given that neuronal responses have a stochastic nature<sup>23</sup>. Since Hubel and Wiesel<sup>17,18</sup> plotted by hand the RFs of neurons in the LGN and striate cortex over 30 years ago, a variety of approaches has been used to map visual RFs quantitatively. Most of these techniques sacrifice resolution along at least one dimension of the RF in order to achieve reasonable data-collection times. In this section, some traditional RF mapping techniques, along with their limitations, are considered briefly and a class of powerful techniques that overcomes these limitations is introduced.

Many studies have characterized RFs using static sensitivity maps, often referred to as 'line-weighting' functions<sup>24,25</sup>. In this approach, a bar (or spot) of light is turned on and off at different positions within the RF, and the average firing rates of a cell to stimulus onset and offset are computed. Because responses are averaged over time, information concerning the temporal structure of the RF is lost. Consequently, static RF profiles are meaningful only if temporal-response properties are independent of spatial position. In some studies, static RF profiles have been derived from responses to moving light and dark bars<sup>26</sup>. This method has the additional disadvantage that spatial and temporal factors are confounded in the RF map.

'Response-plane' techniques<sup>27,28</sup> improve upon static RF maps by measuring the temporal pattern of discharge elicited at each spatial position by a flashing bar (or spot) of light. Although this approach can yield a complete  $x$ - $y$ - $t$  RF map, it is quite slow. For example, consider the task of characterizing a cell's visual sensitivity in  $x$ - $y$ - $t$  by presenting briefly flashed (that is, 50 ms) bright and dark spots at each of  $20 \times 20$  positions in the  $x$ - $y$  plane. To collect 1 s of response following each flash, and to average over ten repetitions of each stimulus, would require a presentation time of more than 2 h. Moreover, studies that have used the response-plane technique<sup>27,28</sup> have typically used flashed stimuli that are too long in duration to reveal

the intrinsic temporal dynamics of a cell's RF (that is, they measure a step response rather than an impulse response).

In recent years, several research groups<sup>3,5,12–15</sup> have developed sophisticated RF-mapping techniques that are based on pseudo-random spatiotemporal stimuli (that is, 'white noise'). White-noise analysis is a general tool for characterizing the input-output behavior of linear and non-linear systems<sup>29,30</sup>. It has a rich history of application in many fields, including retinal electrophysiology<sup>31</sup>. In the white-noise approach to RF mapping, a rapid, pseudo-random stimulus sequence that consists of patterns of spots or bars is presented, and the neuronal spike train is correlated to the stimulus sequence (that is, cross- or reverse-correlation). The aim of this correlation procedure is to characterize the transformation that occurs between the visual stimulus and the response of a neuron (that is, the neuron's 'transfer function'). Because stimuli are presented in rapid succession, without pausing to collect the response to each pattern, this technique is fast. For example, the  $x$ - $y$ - $t$  measurement that is described above, involving  $20 \times 20$  positions and a 50 ms duration, could be accomplished in ~7 min. Theoretical and practical details of this approach are beyond the scope of this paper, and are reviewed elsewhere<sup>32</sup>. For neurons that behave linearly, which is approximately the case for LGN X-cells<sup>33</sup> and cortical simple cells<sup>34,35</sup>, first-order correlations between stimulus and response provide a nearly complete characterization of the RF. For non-linear neurons, such as complex cells<sup>9,21,36</sup>, the manner in which a neuron's response depends on the interactions between stimuli (that is, between different positions or times) must also be considered. Thus, higher-order correlations are needed to characterize fully the RFs of these cells.

### The receptive field as a spatiotemporal entity

The textbook-style depictions of Fig. 1 (left) essentially ignore the temporal dimension of the RF. However, the organization of the RF is not static. In fact, when examined in the space-time domain, the RFs of most cells in the geniculo-cortical pathway exhibit striking dynamics. Given that the RF is a spatio-temporal entity, a fundamental question is that of how space and time interact to determine the properties of a cell's response. There are two basic possibilities: the RF might be space-time separable or it might be inseparable<sup>37,38</sup>. Defined formally, space-time separability means that the three-dimensional RF,  $R(x,y,t)$ , can be described as the product of two independent functions: a spatial profile,  $G(x,y)$ , and a temporal profile,  $H(t)$  [that is,  $R(x,y,t) = G(x,y) \times H(t)$ ]. If a cell's RF is space-time inseparable, it cannot be broken down into spatial and temporal components – a spatio-temporal map is the minimum acceptable descriptor. For these cells, traditional methods of RF mapping, which average responses over time, will not provide an accurate portrait of the RF. The importance of this distinction is illustrated clearly by examining the spatiotemporal RFs of simple cells. Recent studies have shown that simple cell RFs range from separable to strongly inseparable<sup>3,5,13,14</sup>.

Complete spatiotemporal ( $x$ - $y$ - $t$ ) RF profiles are shown in Fig. 2 for representative simple cells from the cat's striate cortex. For the cell of Fig. 2A, the RF is approximately space-time separable. In practical

terms, this means that the spatial arrangement of RF subregions is fixed but their strengths and polarities are modulated over time. For the cell of Fig. 2B, the RF is space-time inseparable, because its spatial organization changes with time. Although there are many possible types of space-time inseparability, simple cells with inseparable RFs exhibit a highly characteristic pattern in which the spatial phase of the RF changes gradually as a function of time<sup>3,8</sup>. When the temporal sequence of RF profiles in Fig. 2B is animated (that is, shown as a movie), subregions of the RF appear clearly to move rightward over time within a tapered spatial window. Note, however, that the two-dimensional spatial envelope of the RF remains approximately fixed as time progresses<sup>3,39</sup>. Not surprisingly, this characteristic form of space-time inseparability has implications for understanding motion selectivity.

### Spatiotemporal RF transformations along the geniculostriate pathway

A convenient way to characterize the dynamics of RF structure is to construct an  $x$ - $t$  plot<sup>13</sup>. An  $x$ - $t$  plot summarizes how the one-dimensional spatial organization of the RF (along the axis perpendicular to the cell's preferred orientation) changes with time. Figure 3 shows  $x$ - $t$  plots for seven representative neurons from the cat's LGN and striate cortex. For LGN cells (Fig. 3A and B), the  $x$ - $t$  plot typically exhibits a center-surround organization in space, and a biphasic structure in time (see also Refs 5 and 6). To a first approximation, the  $x$ - $t$  profiles of LGN cells are space-time separable; however, many LGN cells (for example, Fig. 3A) show two subtle, yet clear, deviations from separability. The temporal response of the surround is often delayed slightly with respect to that of the center. In addition, the first temporal phase of the surround often appears to converge with the second temporal phase of the center, although this second deviation might simply be a consequence of the delayed surround response.

Recent studies have revealed two classes of LGN neurons, lagged and nonlagged, that exhibit different temporal response properties<sup>40,41</sup>. The RFs of lagged cells are distinguished from those of nonlagged cells by a temporal phase shift<sup>42</sup>. For nonlagged cells (Fig. 3A), the first temporal phase of the RF profile is largest, whereas for lagged cells (Fig. 3B), the second temporal phase typically dominates. This property accounts for the delayed response of lagged cells to presentation of a flashed spot stimulus<sup>42</sup>. The temporal properties of lagged cells are thought to arise from intra-geniculate circuitry because lagged responses are not seen in the retina<sup>43</sup>; however, the connectivity that underlies lagged responses remains unclear.

Figure 3C and D shows  $x$ - $t$  plots for simple cells that have approximately space-time separable RFs. These  $x$ - $t$  profiles exhibit multiple lobes in both space and time, and are well approximated by the product of a spatial profile and a temporal profile. Thus, the traditional notion that each cell has a unique spatial RF configuration still pertains to these cells. The spatial profile exhibits typically one to five distinct subregions of alternating polarity, and all possible types of spatial symmetry (that is, spatial phases) are observed<sup>3,44</sup>. The temporal profile is typically biphasic, although some simple cells exhibit either monophasic

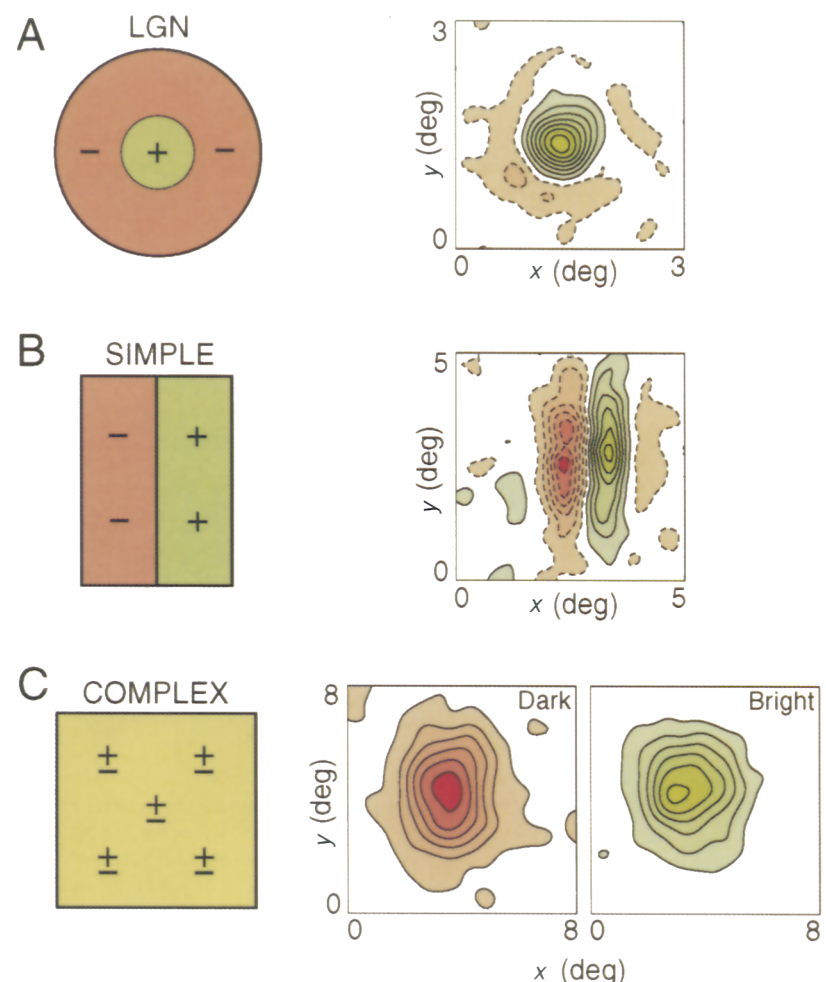


**Fig. 1.** *Spatial receptive field (RF) structure of the major classes of neurons in the geniculostriate pathway.* (A) Schematic and experimental profiles of the RF of an ON-center neuron from the lateral geniculate nucleus (LGN) of a cat. In the traditional depiction (left), the RF has a central 'ON' region (green, +) which is responsive to the onset of a bright stimulus, and a surrounding 'OFF' region (red, -) which is responsive to the onset of a dark stimulus (or the offset of a bright stimulus). On the right is shown a two-dimensional spatial ( $x$ - $y$ ) RF profile for an ON-center X-cell, as measured using a reverse correlation technique<sup>2,3</sup>. Regions of visual space that are responsive to bright spots are shaded green, and are delimited by solid contour lines; regions that are responsive to dark spots are shaded red, and are represented by broken contours. Color saturation is proportional to response strength. A center-surround structure is clearly seen in this profile, although the surround is fairly weak. Similar data have been presented elsewhere for retinal ganglion<sup>4</sup> and LGN (Refs 5–7) cells. (B) Depicted schematically on the left, the RF of a simple cell exhibits an alternating arrangement of elongated subregions that are responsive to either bright (green, +) or dark (red, -) stimuli. A measured RF profile for a simple cell from cat striate cortex (area 17) is shown on the right as a contour map (conventions as in A). Similar data have been presented elsewhere<sup>2,3,5,8</sup>. (C) Spatial RF structure of a complex cell. In the traditional schematic illustration, shown on the left, pluses and minuses are shown throughout the field, indicating that the cell responds to both bright and dark stimuli at each position. Panels on the right show the RF profile of an area 17 complex cell, as measured using reverse correlation (see also Refs 9 and 10). Because regions that are responsive to bright and dark stimuli overlap, separate profiles are shown for bright and dark stimuli.

or triphasic responses<sup>3,8</sup>. Simple cells with multiphasic temporal RF profiles have bandpass temporal frequency tuning, whereas cells with monophasic profiles exhibit low-pass tuning<sup>35</sup>.

Hubel and Wiesel<sup>18</sup> suggested originally that simple cell RFs are created by combining inputs from a group of ON- and OFF-center geniculate neurons with RFs that are arranged in rows, a concept that has received some direct experimental support recently<sup>19</sup>. In this regard, it is interesting to note that the temporal-response pattern within a single subregion of a separable simple-cell RF (Fig. 3C and D) is similar to the

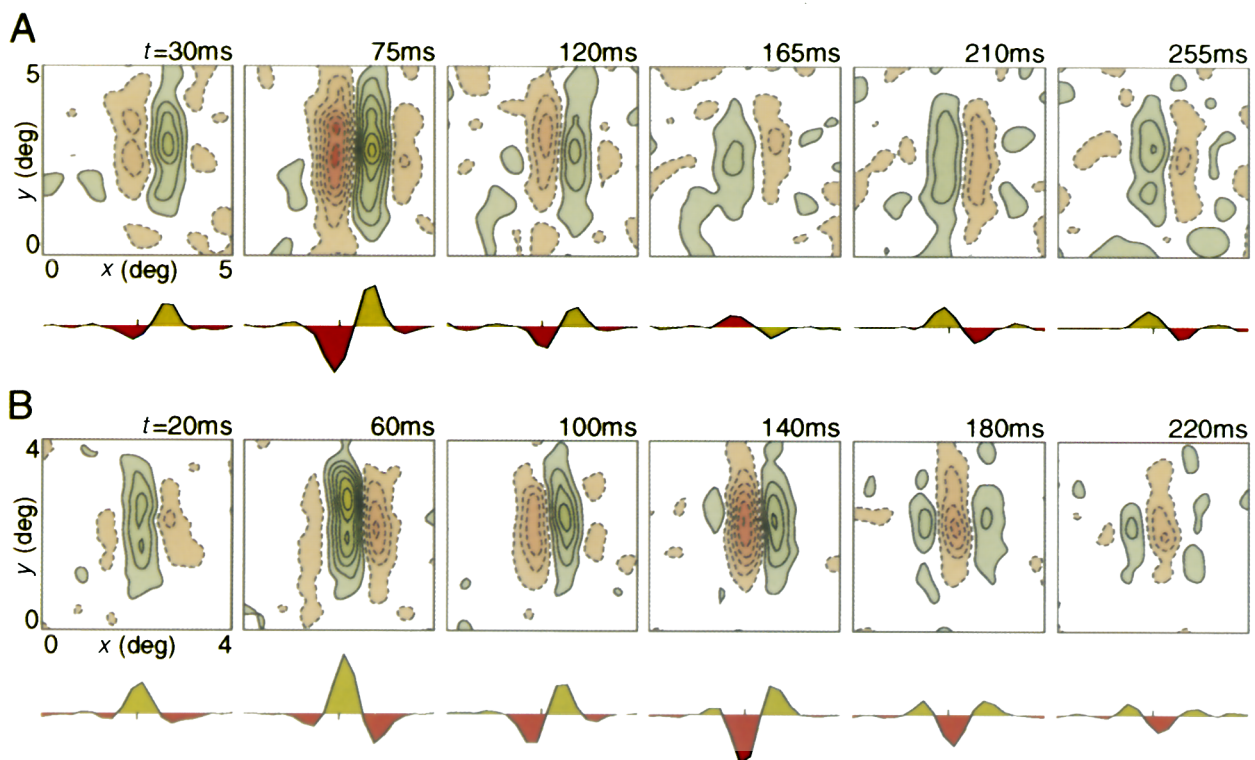


**Fig. 2. Dynamics of receptive field (RF) structure of simple cells from striate cortex of the cat.** By varying the correlation delay,  $t$ , in the RF mapping algorithm, 'snapshots' of the RF can be obtained at different times relative to stimulus onset. These data were obtained using a reverse correlation technique, which is described in considerable detail elsewhere<sup>2,3,8</sup>. For each cell, two-dimensional (2D) spatial ( $x$ - $y$ ) RF profiles are shown, as isoamplitude contour maps (conventions as in Fig. 1), for six values of  $t$ . Below each contour plot is a 1D RF profile that is obtained by integrating the 2D profile along the  $y$  axis, which is parallel to the cell's preferred orientation. Positive deflections (shaded green) in these 1D profiles indicate bright-excitatory subregions; negative deflections (shaded red) correspond to dark-excitatory subregions. Similar data have been presented elsewhere<sup>3,5,8</sup>. (A) The RF of this simple cell is approximately space-time separable. From  $t = 30$  ms to  $t = 120$  ms, the RF profile has two dominant subregions, which are arranged with the dark-excitatory subregion on the left. These subregions are strongest at  $t = 75$  ms. Between  $t = 120$  ms and  $t = 165$  ms, the RF reverses polarity, so that the bright-excitatory subregion is now on the left. This arrangement then persists over the remainder of the cell's response duration. Note that, at all values of  $t$ , the 1D RF profile is approximately odd symmetric (sine phase). (B) A fundamentally different type of spatiotemporal behavior is illustrated here. For this cell, the RF is space-time inseparable – the spatial organization of the RF changes over time. At  $t = 20$  ms, the 1D profile is approximately even symmetric (cosine phase) whereas, at  $t = 100$  ms, the RF profile is odd symmetric. Later, at  $t = 180$  ms, the RF becomes even symmetric again but the profile is inverted relative to that at  $t = 20$  ms.

temporal structure that is observed within the RF center of either an ON- or OFF-center LGN cell (Fig. 3A). Thus, the temporal organization of separable simple-cell RFs seems consistent with the idea that these RFs could be constructed from arrays of LGN fields.

Unlike LGN neurons, however, a majority of simple cells exhibit marked space-time inseparability<sup>3,8</sup>. Two such examples are shown in Fig. 3E and F. The  $x$ - $t$  plots for these cells exhibit bright- and dark-excitatory subregions that are tilted in the space-time domain. Consequently, there is no unique spatial (or temporal) RF profile, because bright- and dark-excitatory subregions move as a function of time. Clearly, for these cells, the definition of a RF must incorporate both space and time.

An important unresolved question concerns the neuronal circuitry by which space-time inseparable RFs are constructed. This process must take place within striate cortex, because LGN cells do not exhibit tilted subregions in their  $x$ - $t$  plots. One suggestion is that inseparable simple-cell RFs are constructed from a pair of separable simple-cell RFs that are arranged in spatial and temporal quadrature<sup>37,45</sup>. Another idea is that inseparable RFs are constructed directly from a combination of lagged and nonlagged geniculate inputs to the cortex<sup>46</sup>. Receptive-field maps of correlated dis-

charge<sup>47</sup> between simultaneously recorded LGN and simple cells might help to differentiate between these schemes, since the latter scheme predicts the existence of simple cells with inseparable RFs that receive monosynaptic input from the LGN, whereas the former scheme predicts that monosynaptically driven simple cells should have separable RFs.

Thus far, the response properties of LGN and simple cells, for which first-order\* RF profiles provide a fairly complete description, have been considered. For complex cells, which exhibit overtly non-linear spatial summation<sup>18,21</sup>, this is not the case. Figure 3G shows  $x$ - $t$  plots of the responses of a complex cell to bright and dark stimuli (first-order RF profiles). Note that the bright- and dark-responsive regions overlap almost completely in the space-time domain, and there are no distinct subregions visible within either domain. Although they define the spatiotemporal envelope of the RF, these first-order RF profiles have little predictive power for determining the response of a complex cell to an arbitrary stimulus<sup>36</sup>. However, second-order RF profiles, which reveal non-linear interactions

\*The terms *first-order* and *second-order* are used to refer to RF profiles that are derived by computing the cross-correlation between a cell's response and either a single stimulus or a pair of stimuli, respectively.

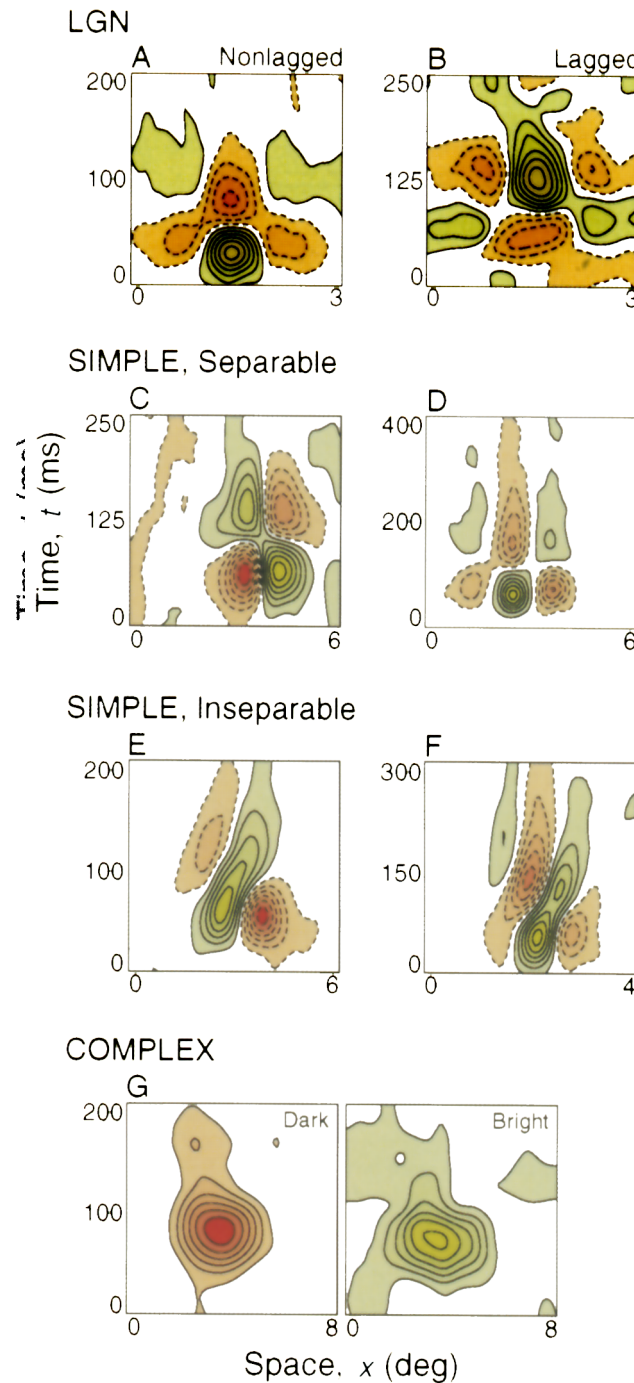
**Fig. 3.** Spatiotemporal receptive field (RF) profiles ( $x$ - $t$  plots) for neurons recorded from the lateral geniculate nucleus (LGN) and striate cortex of the cat. In each panel, the horizontal axis represents space ( $x$ ), and the vertical axis represents time ( $t$ ). For panels A–F, solid contours (with green shading) delimit bright-excitatory regions, whereas broken contours (with red shading) indicate dark-excitatory regions. To construct these  $x$ - $t$  plots, 1D RF profiles (see Fig. 2) are obtained, at finely spaced time intervals (5–10 ms), over a range of values of  $t$ . These 1D profiles are then ‘stacked up’ to form a surface, which is smoothed and plotted as a contour map (for details, see Refs 3 and 8). (A) An  $x$ - $t$  profile is shown here for a typical ON-center, non-lagged X-cell from the LGN. For  $t < 50$  ms, the RF has a bright-excitatory center and a dark-excitatory surround. However, for  $t > 50$  ms, the RF center becomes dark-excitatory, and the surround becomes bright-excitatory. Similar spatiotemporal profiles are presented elsewhere<sup>5,6</sup>. (B) An  $x$ - $t$  plot of an ON-center, lagged X-cell. Note that the second temporal phase of the profile is strongest. (C) An  $x$ - $t$  profile for a simple cell with a space-time separable RF. For  $t < 100$  ms, the RF has a dark-excitatory subregion to the left of a bright-excitatory subregion. For  $t > 100$  ms, each subregion reverses polarity, so that the bright-excitatory region is now on the left. Similar  $x$ - $t$  data are presented elsewhere<sup>3,8,35</sup>. (D) Data for another simple cell with an approximately separable  $x$ - $t$  profile. (E) Data are shown for a simple cell with a clearly inseparable  $x$ - $t$  profile. Note how the spatial arrangement of bright- and dark-excitatory subregions (that is, the spatial phase of the RF) changes gradually with time (see Refs 3, 5, 8, 13 and 35 for similar data). (F) An inseparable  $x$ - $t$  profile is shown here for the same simple cell for which 2D spatial profiles are shown in Fig. 2B. Note that the subregions are tilted to the right in the space-time domain. (G)  $x$ - $t$  profiles are shown for the same complex cell as in Fig. 1C (see also Ref. 9). Responses to bright and dark stimuli are shown separately because these regions overlap extensively.

between stimuli presented at different positions or times, have a spatiotemporal organization that is reminiscent of the first-order profiles of simple cells<sup>12,22,36</sup>. These second-order RF profiles are thought to represent the structure of subunits that are combined to form a complex cell’s RF. Gaska and colleagues<sup>36</sup> have shown recently that second-order RF profiles provide accurate predictions of the orientation, spatial frequency, and direction selectivity of complex cells in the monkey.

#### Spatiotemporal mechanisms that underlie motion selectivity

Recent studies of RF dynamics have provided a greater understanding of the mechanisms that underlie motion selectivity. Unlike their geniculate antecedents, most cortical neurons are quite selective for stimulus velocity (that is, direction and speed). In the geniculostriate pathway of cats and monkeys, neurons that are strongly selective for direction of motion are encountered commonly in the striate cortex<sup>18,48</sup>, whereas X- and Y-type relay cells in the LGN seldom exhibit more than a weak directional bias<sup>49</sup>. The speed tuning of cortical neurons is also much narrower than that of LGN cells<sup>50</sup>.

What accounts for the striking directional selectivity of many cortical neurons? Despite an abundance of studies, a consensus regarding the mechanistic underpinnings of direction selectivity has emerged only recently. Hubel and Wiesel<sup>18</sup> suggested initially that direction selectivity in simple cells could be explained on the basis of the arrangement of ON and OFF subregions within the RF. However, subsequent studies revealed that these predictions often fail<sup>51,52</sup>. Thus, until about ten years ago, it was widely held that direction selectivity originates via non-linear interac-



tions, typically involving delayed excitation or inhibition between different parts of the RF (Refs 53 and 54).

More recently, theoretical<sup>37,45</sup> and psychophysical<sup>55</sup> studies have suggested that direction selectivity originates in the linear (that is, first order) spatiotemporal RF structure of simple cells. Specifically, simple cells with RF profiles that are tilted (that is, inseparable) in the space-time domain (Fig. 3E and F) are expected to exhibit a directional preference, whereas cells with space-time separable RFs are not. Recent studies have largely confirmed this prediction. A simple cell’s preferred direction of motion can be predicted reliably from the structure of its  $x$ - $t$  profile<sup>8,35</sup>. Moreover, accurate estimates of the preferred speed of motion can be derived by measuring the slope of oriented subregions in the  $x$ - $t$  profile<sup>8,13</sup>. These findings support the idea that linear spatiotemporal mechanisms underlie velocity selectivity (similar conclusions have also been

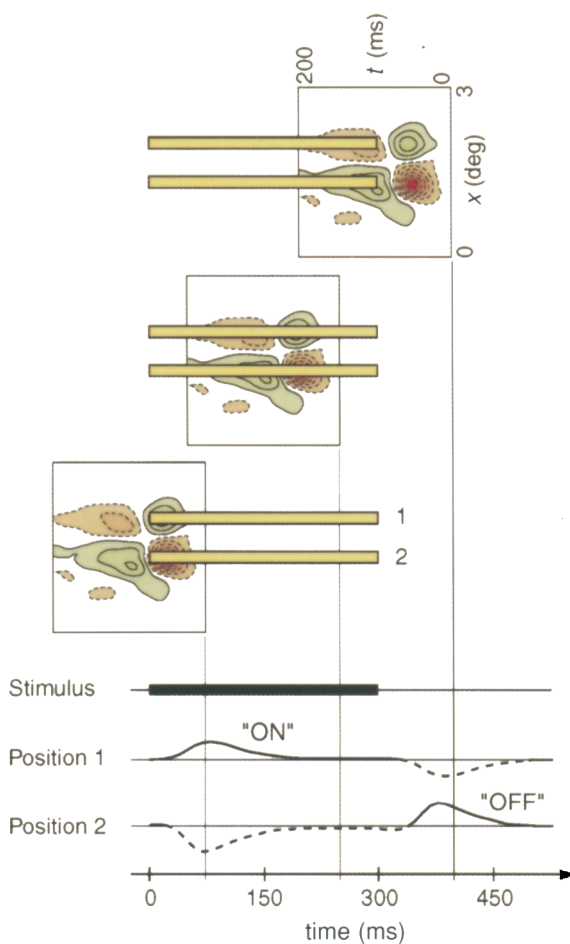


**Fig. 4. Relationship between  $x$ - $t$  profile and ON/OFF responses.** Simulation of the response of a simple cell to a sustained flash of a bar stimulus at two different positions (1 and 2) within the receptive field (RF). (Top.) Illustration, in a space-time coordinate frame, of the convolution process that is used to predict the response to a 300 ms flash of a bright bar. The flashed-bar stimulus is represented as a horizontal rectangle (yellow) in the space-time domain. The cell's response is predicted by sliding the RF profile from left to right (three time frames from this sliding process are illustrated). At each time interval, the predicted response is given by the net volume of the  $x$ - $t$  data that lie under the bar stimulus, with bright- and dark-excitatory areas weighted positively and negatively, respectively<sup>57</sup>. The convolution process that is used here is based on the assumption of linear spatiotemporal summation, which holds reasonably well for most simple cells<sup>35</sup>. Known non-linearities, such as an expansive exponent<sup>56</sup> or contrast normalization<sup>58</sup>, would modify the shape of the predicted responses, but not the basic ON/OFF pattern. (Bottom.) Smooth curves show predicted responses of the cell to a flashed bright bar at positions 1 and 2. Broken portions of the curves indicate inhibitory responses which, generally, cannot be observed in the spike train of simple cells, owing to a lack of spontaneous discharge. At position 1, there is an excitatory response after stimulus onset, whereas position 2 exhibits an excitatory discharge at stimulus offset. Note that, if a dark bar is flashed over the RF instead of a bright bar, the polarity of the predicted responses will be reversed, so that position 1 gives an OFF response and position 2 gives an ON response. Thus, the ON/OFF classification scheme is dependent upon stimulus polarity.

reached by making measurements in the frequency domain<sup>38,56</sup>.

Although the directional selectivity of simple cells has its basis in linear RF structure, contrast-related non-linearities appear to play a role in enhancing this selectivity. Typically, linear predictions underestimate the degree of direction selectivity that is observed in the responses of simple cells to drifting gratings<sup>35,38,56</sup>.

However, these discrepancies can be accounted for largely by two non-linear aspects of a cell's response to different contrasts – an expansive exponent and contrast gain control<sup>35,56,57</sup>. These non-linearities accentuate the directional bias that originates in the linear spatiotemporal structure of the RF.

For complex cells, many of which are also direction-selective, first-order RF profiles (Fig. 3G) cannot predict velocity tuning. For these cells, however, spatio-temporally oriented RF subregions are revealed clearly in second-order RF profiles, which are obtained by probing non-linear interactions between different positions and times within the RF (Refs 12 and 36). These second-order RF profiles can be used to make accurate predictions of a complex cell's tuning characteristics, including its direction selectivity<sup>36</sup>. Moreover, these second-order profiles are consistent with those that are predicted by a motion-energy model<sup>9</sup>, in which the complex-cell RF is constructed from a non-linear combination of simple-like RFs that are space-time inseparable. The non-linear response properties of complex cells appear to make them well suited to signal local image velocity independently of other factors, such as contrast polarity and spatial phase, that are confounded in the responses of simple cells.

#### Origin of ON and OFF responses

Because spatiotemporal RF maps are relatively new to visual neurophysiology, it is important to clarify how the organization of  $x$ - $t$  profiles relates to the traditional ON/OFF classification scheme. The RFs of visual neurons are usually described in terms of 'ON' and 'OFF' responses, which are discharges that occur at the onset or offset, respectively, of a spot of light. Simple-cell and LGN RFs have spatially segregated ON and OFF subregions, whereas complex-cell RFs do not<sup>18</sup>.

Because the  $x$ - $t$  profile provides an almost complete description of the response properties of most simple cells, the relationship between spatiotemporal RF profiles and the traditional ON/OFF classification scheme can be explored by making linear predictions of the response of a simple cell to a conventional stimulus. Figure 4 shows predicted responses of a simple cell, with a space-time separable RF, to a bar of light that is flashed at one of two positions within the RF. At position 1, the cell's  $x$ - $t$  profile has a bright-excitatory phase followed by a dark-excitatory phase; this configuration yields an 'ON' response to the flashed bar. At position 2, the RF has a dark-excitatory phase followed by a bright-excitatory phase, resulting in an 'OFF' response to the same stimulus. Note that the biphasic nature of this cell's RF profile is essential to the generation of an OFF response at position 2. However, it must be emphasized that the second temporal response phase of the  $x$ - $t$  profile does not represent an offset response to the mapping stimuli. The biphasic temporal-response pattern that is exhibited by most LGN and simple cells is an intrinsic property of these neurons, and does not result from 'mixed ON/OFF regions', as suggested recently<sup>5</sup>. Thus, although ON and OFF responses can be predicted from the  $x$ - $t$  profile, the converse is not true.

This point is further illustrated by Fig. 5A, which shows predicted responses of a simple cell that has a space-time inseparable RF. Response predictions at three different spatial positions illustrate that the RF

can be approximately parcelled into two 'ON' regions, with an 'OFF' region in between (Fig. 5A, right). This simulation might explain why earlier studies<sup>18,28</sup>, using the ON/OFF classification, did not distinguish between simple cells that have separable and inseparable RFs. Although the ON/OFF map can be derived from the  $x-t$  profile, the ON/OFF description is not complete, nor is it unique. For example, a simple cell's velocity selectivity can be predicted from the  $x-t$  profile<sup>8,35</sup> but not from the ON/OFF map.

In some cases, ON/OFF classification of RF structure can give erroneous results. Figure 5B shows data for a simple cell with a RF profile that is bipartite in space, and monophasic in time. The predicted response to a bright bar at position 1 shows a sustained period of excitation, beginning just after stimulus onset and terminating at stimulus offset. This can be considered an ON response. At position 2, there is a sustained inhibitory response that is usually not observable due to a lack of spontaneous discharge<sup>28</sup>. There is no OFF response to a bright bar at position 2, although there is a dark-excitatory subregion here. Hence, the size and periodicity of the RF might be underestimated when testing with only a bright bar, because a dark-excitatory subregion is not equivalent to an OFF region.

### Concluding remarks

In this review, a systems-analysis approach to characterizing the response properties of neurons in the central visual pathways has been considered. The essence of this approach is to obtain a complete description of the input–output relationship of a neuron (that is, its RF profile) by testing it with a rich, spatiotemporal stimulus ('white noise'). By extending the traditional description of visual RFs into the joint space–time ( $x-y-t$ ) domain, recent studies of RF dynamics have provided new information about mechanisms of visual-information processing in the geniculostriate pathway. An inescapable conclusion of these studies is that the RF must be treated as a spatiotemporal entity. For cells with space–time inseparable RFs, a spatiotemporal response profile is the minimum acceptable descriptor, because there is no unique spatial (or temporal) RF profile.

Future work will undoubtedly extend the description of visual RFs even further. In this review, for example, we have only considered the responses of neurons to monocular stimulation. However, because most neurons in the striate cortex receive binocular input<sup>18</sup>, a complete description of these RFs involves consideration of a fourth dimension: depth (or binocular disparity),  $z$ . A description of RFs in the  $x-y-z-t$  domain awaits further research, although recent work has made important strides toward this goal<sup>10</sup>.

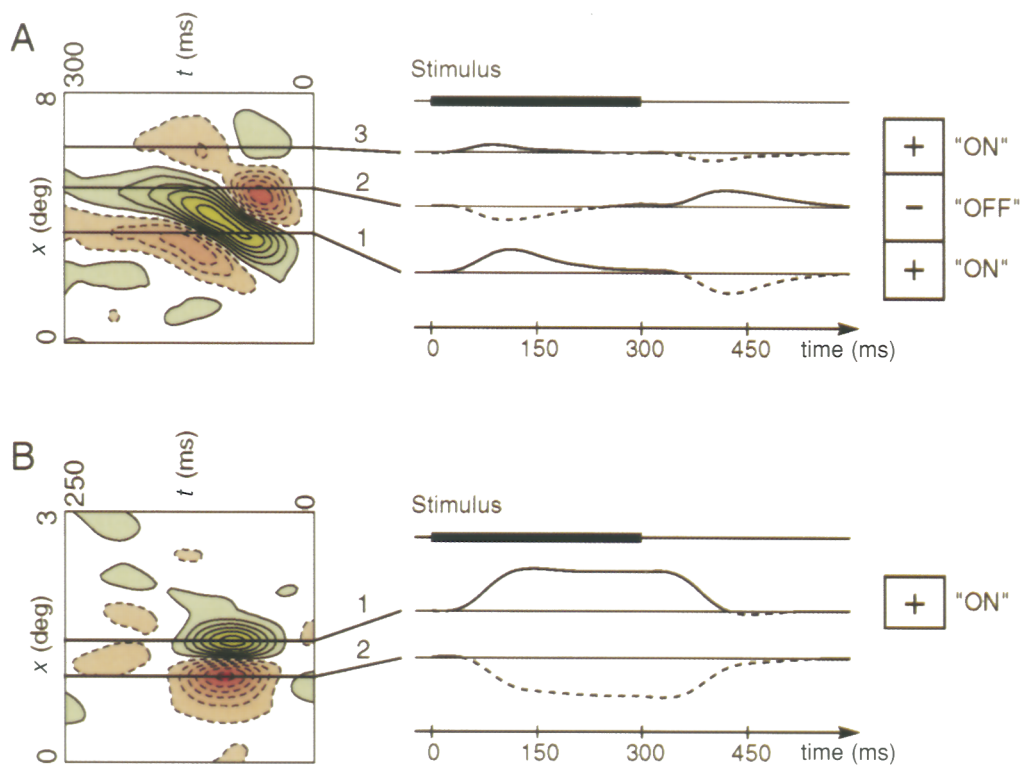


**Fig. 5.** Predicted responses of two simple cells to a sustained flash of a bar of light (computed as described in Fig. 4). (A) This simple cell has a space–time inseparable receptive field (RF). The cell gives an 'ON' response at positions 1 and 3, and an 'OFF' response at position 2. A traditional-style ON/OFF map of the RF is shown on the right. (B) The RF of this simple cell is monophasic along the time dimension. There is a sustained 'ON' response at position 1 but no observable (that is, excitatory) response at position 2. Thus, traditional ON/OFF mapping with only a bright bar would produce an incomplete RF map (right). Note that the dark-excitatory subregion will be observable in the ON response to a sustained flash of a dark bar stimulus at position 2. However, many previous studies have mapped cortical RFs using only bright bars or spots.

In principle, white-noise analysis can provide a complete characterization of the behavior of any non-linear system<sup>29,30</sup>. However, it is worth noting that successful application of these methods has thus far been limited to the study of neurons in the early portions of the visual pathway, for which response properties are well described in terms of first- and second-order correlations. For neurons in higher visual areas, the increasing complexity of organization of RFs is likely to necessitate the measurement of higher-order correlations, thus requiring longer recording times. Moreover, owing to practical considerations in the design of experiments, there might be important determinants of neuronal selectivity that are not represented in spatiotemporal RF maps. For example, because white-noise mapping is usually performed at a fixed contrast level, dynamic non-linearities such as contrast gain control<sup>59</sup> might be overlooked. To obtain a complete input–output description for a neuron, one must have access to all of the relevant inputs. This might prove to be problematic for studying neurons in extra-striate cortical areas, where extra-retinal factors such as attention, memory, and eye position often modulate neuronal responses<sup>60</sup>. Despite these considerations, however, white-noise analysis has considerable potential for elucidating the details of RF structure at higher levels in the visual pathway.

### Selected references

- 1 Hartline, H.K. (1940) *Am. J. Physiol.* 130, 690–699
- 2 Jones, J.P. and Palmer, L.A. (1987) *J. Neurophysiol.* 58, 1187–1211

## Acknowledgements

This work was supported by research and CORE grants from NIH (EY01175 and EY03176), and by a collaborative project of the Human Frontiers Science Program.

The authors are grateful to Akiyuki Anzai, Daqing Cai and Geoff Ghose for assisting with experiments, and for providing helpful comments on the manuscript.

The authors also thank David Heeger for suggesting the graphical representation used in Fig. 4.

- 3 DeAngelis, G.C., Ohzawa, I. and Freeman, R.D. (1993) *J. Neurophysiol.* 69, 1091–1117
- 4 Citron, M.C., Emerson, R.C. and Levick, W.R. (1988) *Ann. Biomed. Eng.* 16, 65–77
- 5 Eckhorn, R., Krause, F. and Nelson, J.I. (1993) *Biol. Cybern.* 69, 37–55
- 6 Golomb, D. et al. (1994) *J. Neurophysiol.* 72, 2990–3003
- 7 Reid, R.C. and Shapley, R.M. (1992) *Nature* 356, 716–718
- 8 McLean, J., Raab, S. and Palmer, L.A. (1994) *Visual Neurosci.* 11, 271–294
- 9 Emerson, R.C., Bergen, J.R. and Adelson, E.H. (1992) *Vision Res.* 32, 203–218
- 10 Ohzawa, I., DeAngelis, G.C. and Freeman, R.D. (1990) *Science* 249, 1037–1041
- 11 Citron, M.C. and Emerson, R.C. (1983) *Brain Res.* 279, 271–277
- 12 Emerson, R.C. et al. (1987) *J. Neurophysiol.* 58, 33–65
- 13 McLean, J. and Palmer, L.A. (1989) *Vision Res.* 29, 675–679
- 14 Shapley, R.M. and Reid, R.C. (1991) in *Computational Models of Visual Processing* (Landy, M.S. and Movshon, J.A., eds), pp. 109–118, MIT Press
- 15 Jacobson, L.D. et al. (1993) *Vision Res.* 33, 609–626
- 16 Kuffler, S.W. (1953) *J. Neurophysiol.* 16, 37–68
- 17 Hubel, D.H. and Wiesel, T.N. (1961) *J. Physiol.* 155, 385–398
- 18 Hubel, D.H. and Wiesel, T.N. (1962) *J. Physiol.* 160, 106–154
- 19 Chapman, B., Zahs, K.R. and Stryker, M.P. (1991) *J. Neurosci.* 11, 1347–1358
- 20 Ferster, D. and Koch, C. (1987) *Trends Neurosci.* 10, 487–492
- 21 Movshon, J.A., Thompson, I.D. and Tolhurst, D.J. (1978) *J. Physiol.* 283, 79–99
- 22 Szulborski, R.G. and Palmer, L.A. (1990) *Vision Res.* 30, 249–254
- 23 Shadlen, M.N. and Newsome, W.T. (1994) *Curr. Opin. Neurobiol.* 4, 569–579
- 24 Baker, C., Jr and Cynader, M.S. (1986) *J. Neurophysiol.* 55, 1136–1152
- 25 Field, D.J. and Tolhurst, D.J. (1986) *Proc. R. Soc. London Ser. B* 228, 379–400
- 26 Kulikowski, J.J., Bishop, P.O. and Kato, H. (1981) *Exp. Brain Res.* 44, 371–385
- 27 Stevens, J.K. and Gerstein, G.L. (1976) *J. Neurophysiol.* 39, 213–238
- 28 Palmer, L.A. and Davis, T.L. (1981) *J. Neurophysiol.* 46, 260–276
- 29 Marmarelis, P.Z. and Marmarelis, V.Z. (1978) *Analysis of Physiological Systems*, Plenum
- 30 Schetzen, M. (1980) *The Volterra and Wiener Theories of Nonlinear Systems*, Wiley
- 31 Sakai, H.M. (1992) *Physiol. Rev.* 72, 491–505
- 32 Victor, J.D. (1992) in *Nonlinear Vision: Determination of Neural Receptive Fields, Function, and Networks* (Pinter, R.B. and Nabet, B., eds), pp. 1–38, CRC Press
- 33 Hochstein, S. and Shapley, R.M. (1976) *J. Physiol.* 262, 237–264
- 34 Movshon, J.A., Thompson, I.D. and Tolhurst, D.J. (1978) *J. Physiol.* 283, 53–77
- 35 DeAngelis, G.C., Ohzawa, I. and Freeman, R.D. (1993) *J. Neurophysiol.* 69, 1118–1135
- 36 Gaska, J.P. et al. (1994) *Visual Neurosci.* 11, 805–821
- 37 Adelson, E.H. and Bergen, J.R. (1985) *J. Opt. Soc. Am. A* 2, 284–299
- 38 Reid, R.C., Soodak, R.E. and Shapley, R.M. (1991) *J. Neurophysiol.* 66, 505–529
- 39 McLean, J. and Palmer, L.A. (1994) *Visual Neurosci.* 11, 295–306
- 40 Mastronarde, D.N. (1987) *J. Neurophysiol.* 57, 357–380
- 41 Humphrey, A.L. and Weller, R.E. (1988) *J. Comp. Neurol.* 268, 429–447
- 42 Saul, A.B. and Humphrey, A.L. (1990) *J. Neurophysiol.* 64, 206–224
- 43 Mastronarde, D.N. (1987) *J. Neurophysiol.* 57, 381–413
- 44 Hamilton, D.B., Albrecht, D.G. and Geisler, W.S. (1989) *Vision Res.* 29, 1285–1308
- 45 Watson, A.B. and Ahumada, A., Jr (1985) *J. Opt. Soc. Am. A* 2, 322–341
- 46 Saul, A.B. and Humphrey, A.L. (1992) *J. Neurophysiol.* 68, 1190–1208
- 47 Ghose, G.M., Ohzawa, I. and Freeman, R.D. (1994) *J. Neurophysiol.* 71, 330–346
- 48 Schiller, P.H., Finlay, B.L. and Volman, S.F. (1976) *J. Neurophysiol.* 39, 1288–1319
- 49 Thompson, K.G., Zhou, Y. and Leventhal, A.G. (1994) *Visual Neurosci.* 11, 927–938
- 50 Movshon, J.A. (1975) *J. Physiol.* 249, 445–468
- 51 Heggenlund, P. (1984) *Vision Res.* 24, 13–16
- 52 Peterhans, E., Bishop, P.O. and Camarda, R.M. (1985) *Exp. Brain Res.* 57, 512–522
- 53 Barlow, H.B. and Levick, W.R. (1965) *J. Physiol.* 178, 477–504
- 54 Ruff, P.I., Rauschecker, J.P. and Palm, G. (1987) *Biol. Cybern.* 57, 147–157
- 55 Burr, D.C., Ross, J. and Morrone, M.C. (1986) *Proc. R. Soc. London Ser. B* 227, 249–265
- 56 Albrecht, D.G. and Geisler, W.S. (1991) *Visual Neurosci.* 7, 531–546
- 57 Heeger, D.J. (1993) *J. Neurophysiol.* 70, 1885–1898
- 58 Heeger, D.J. (1992) *Visual Neurosci.* 9, 181–197
- 59 Ohzawa, I., Sclar, G. and Freeman, R.D. (1985) *J. Neurophysiol.* 54, 651–667
- 60 Maunsell, J.H. and Newsome, W.T. (1987) *Annu. Rev. Neurosci.* 10, 363–401

## In the other Trends journals

A short selection of articles that might be of interest to our readers.

**Novel dopamine receptors half a decade later**, by P. Sokoloff and J-C. Schwartz  
*Trends in Pharmacological Sciences* 16, 270–275

**Fishing for drugs from the sea: status and strategies**, by D.J. de Vries and P.M. Beart  
*Trends in Pharmacological Sciences* 16, 275–279

**Is NSF a fusion protein?**, by Alan Morgan and Robert D. Burgoyne  
*Trends in Cell Biology* 5, 335–339

**mRNA translocation and microtubules: insect ovary models**, by Howard Stebbings, Jonathan D. Lane and Nicholas J. Talbot  
*Trends in Cell Biology* 5, 361–365

**A mitochondrial bottleneck hypothesis of Alzheimer's disease**, by John N. Davis, Edward J. Hunnicutt, Jr and Jane C. Chisolm  
*Molecular Medicine Today* 1, 240–247

**Representational difference analysis: finding the differences between genomes**, by Nikolai A. Lisitsyn  
*Trends in Genetics* 11, 303–307

**Retinoic acid and pattern formation in vertebrates**, by Ronald A. Conlon  
*Trends in Genetics* 11, 314–319

**Using GFP to see the light**, by Douglas C. Prasher  
*Trends in Genetics* 11, 320–323